Article

Not peer-reviewed version

Increasing SBA-15 Amphoteric Properties by Direct Zr Addition During Synthesis

Romeo Hernández-Morales , José Escobar * , José Guadalupe Pacheco-Sosa , José Gilberto Torres-Torres , David S. García-Zaleta , Zenaida Guerra-Que , Paz Del Angel Vicente , María C. Barrera , Durvel de la Cruz-Romero

Posted Date: 31 October 2024

doi: 10.20944/preprints202410.2582.v1

Keywords: Zirconia; SBA-15; amphoteric properties; surface acidity-basicity

 doi:10.20944/preprints202410.2582.v1

Article

Increasing SBA-15 Amphoteric Properties by Direct Zr Addition During Synthesis

Romeo Hernández [1], José Escobar [2,*], José G. Pacheco [1], José G. Torres [1], David S. García [3], Zenaida Guerra [4], Paz del Ángel [2], María C. Barrera [5] and Durvel de la Cruz [1]

[1] Universidad Juárez Autónoma de Tabasco (UJAT), División Académica de Ciencias Básicas, Cunduacán, Tabasco, 86690, México.
[2] Instituto Mexicano del Petróleo, Eje Central Lázaro Cárdenas Norte 152, San Bartolo Atepehuacan, G.A. Madero, Cd. de México, 07730, México.
[3] Universidad Juárez Autónoma de Tabasco (UJAT), División Académica Multidisciplinaria de Jalpa de Méndez, Carretera Estatal Libre Villahermosa – Comalcalco km 27+000 s/n Ranchería Ribera Alta, Jalpa de Méndez, Tabasco, 86205, México.
[4] Tecnológico Nacional de México-Instituto Tecnológico de Villahermosa (TECNM – I. T. Villahermosa), Laboratorio de Investigación 1 Área de Nanotecnología, km. 3.5 Carretera Villahermosa-Frontera, Cd. Industrial, Villahermosa, Tabasco, 86010, México.
[5] Universidad Veracruzana, Campus Coatzacoalcos, Facultad de Ciencias Químicas, Av. Universidad km. 7.5, Col. Santa Isabel, Coatzacoalcos, Veracruz, 96538, México.
* Correspondence: Corresponding: jeaguila@imp.mx

Abstract Strategies followed to improve SBA-15 surface (essentially inert) included modifications by adding acidic or basic (or both) species during or after silica synthesis. Amphoteric properties are especially important as some reactions (alcohols dehydrations, for instance) require of both type of sites to efficiently take place. In this work, single Zr (nominal 3, 5 and 10 wt%, as $ZrOCl_2 \bullet 8H_2O$) direct addition during SBA-15 synthesis was used to impart amphoteric characteristics (as determined by NH_3 and CO_2 TPD) to mesostructured SiO_2 matrices. Additional materials characterization included textural (N_2 physisorption) and structural (XRD, FTIR and UV-vis spectroscopies, and HRTEM as well) studies. Actual solids composition was also determined (EDS). Degree of Zr incorporation to mesoporous silica was enhanced with nominal content in binary formulations, although not necessarily integrated in SBA-15 walls forming Zr-O-Si linkages. It seemed that single ZrO_2 domains (framework and extra-framework) could provide suitable amphoteric properties by significantly increasing number and strength of both acid and basic sites (especially formulation containing nominal 5 wt% Zr), as to those over mesostructured silica matrices. Also, potentially deleterious strong acid sites were avoided. The binary oxides present great potential to be applied in reactions requiring vicinal acid-basic pairs (alcohols dehydration, for instance).

Keywords Zirconia; SBA-15; amphoteric properties; surface acidity-basicity

1. Introduction

Amphoteric solids could play a decisive role in improving activity, selectivity and stability of catalytic materials. Over those bifunctional formulations new reaction pathways of well-known reactions could be provided and improved yields of desired products could be achieved. For instance, sol-gel ZrO_2 and corresponding Na-modified solids catalysts effectively cleaved the β-ether bond of phenethyl phenyl ether (from biomass-derived lignin valorization) to produce ethyl benzene, styrene and phenol as major products [1]. Followed reaction pathways and thus product distribution were correlated to concentration of both surface acid (Lewis) and basic sites on the studied materials. Even more, some reactions require participation of both type of sites to take place. Otherwise, they could not be carried out at all on either acid or basic centers alone, for instance, aldol condensation between 4-nitrobenzaldehyde and acetone, where also acid strength played a major role [2]. In this context, functionalization of rather inert SBA-15 mesoporous silica have been tried for some groups by using inorganic oxides [3-4]. Even organic species have been used to that end [2, 5]. SBA-15 materials

 doi:10.20944/preprints202410.2582.v1

possess very good textural properties (large surface area, high pore volume, mesoporosity) that could be tuned depending on synthesis conditions used but lack both acidity and basicity [6]. Different strategies followed to improve surface properties have included modifications by adding Al and Mg salts during synthesis [3], species that could provide (after calcination) Lewis or protonic acidity (depending on Al^{3+} location. framework or extra-framework [7]) and basic sites (as MgO). Zirconium and magnesium salts direct addition during direct mesoporous silica matrix formation have also been utilized to that end, by creation of acidic and basic domains, respectively, [4]. Considering zirconia surface amphoteric properties [8], in this investigation a simpler approach was studied, i. e, direct addition during SBA-15 synthesis [9] of Zr salt alone. The main focus was determining if that strategy could provide enhanced acid and basic sites population on otherwise inert SiO_2 surface. Binary solids at various Zr content prepared through methodology used in [10] (substituting Ti for Zr), were studied and characterized by textural, structural and surface instrumental techniques. Being a critical parameter that could strongly influence correct analytical data interpretation [6], actual materials composition was also determined. As in previous reports, those sites were analyzed through ammonia and CO_2 thermodesorption. It seems that ZrO_2 domains alone could provide desired amphoteric characteristics to mesostructured silica matrices.

2. Results and Discussion

2.1. Materials Composition

According to data in Table 1, degree of Zr incorporation in SBA-15 improved as the intended modifier concentration augmented. Probably, Zr species when at lower amount were not well-integrated to mesoporous framework. could be dissolved during washing of gel precursor [6]. Originally, SBA-15 solid modified by 1 wt% Zr was also prepared but chemical analysis failed to identify zirconium domains in corresponding sample. This solid was then not further studied. Otherwise, when at higher concentration, Zr polymeric species of lower solubility could be formed [11] remaining after gel washing. It is worth nothing that those extant Zr domains could not necessarily be properly integrated in SiO_2 tetrahedral network. In the case of SBA-15 modified by MgO and ZrO_2 Chen net al. [4] identified Zr in the SBA-15 matrix by EDS but, unfortunately no quantitative data were provided making impossible to determine the amount of zirconia in the solid (20 wt% of equimolar ZrO_2/MgO).

Table 1. EDS analyses of prepared materials at various nominal Zr contents.

Sample	O (wt%)	Si (wt%)	Zr (wt%)
S	45.19	38.95	--
Z3S	45.65	53.94	0.41
Z5S	45.79	50.95	3.26
Z10S	45.06	46.40	8.54

2.2. Materials Texture

Although SBA-15 pristine matrix and corresponding Zr-modified materials all had type IV N_2 adsorption isotherms (Figure S1 (a)) with H1 hysteresis, typical profiles of mesostructured solids with cylindrical pores [12], they showed distinctive features when compared one to another. Z3S displayed notably increased adsorbed N_2 volume meanwhile Z10S exhibited very marked hysteresis strongly suggesting presence of ink-bottle shaped pores. Thus, important textural alterations in studied samples could be envisaged. Z3S was the solid of the highest surface area (20% larger as to that of pristine SBA-15) where no definite trend related to modifier content was observed (Table S1). Pore volume remained unaltered by Zr addition but in the Z3S case which had strongly increased one (56%), respecting pristine mesoporous silica. As suggested by shifts to lower or higher partial

 doi:10.20944/preprints202410.2582.v1

pressures closing of their hysteresis (as to that of SBA-15), for Z10S and Z3S smaller and higher average pore size than that of S were registered (see corresponding maxima in Table S1 and Figure S1(b)). All in all, textural parameters suggested that certain pore obstruction were provoked in Z10S due to augmented Zr species content whereas the highest ZrO_2-SBA-15 interaction was expected in Z3S.

2.3. X-Ray Diffraction

Wide humps in the ~15-35° 2θ range in diffractograms of studied binary oxides (Figure S2) corresponded to amorphous mesoporous silica walls [13]. Absence of diffraction signals related to zirconia phases (monoclinic one, according to annealing temperature samples were submitted to [14]) suggested amorphous domains of well-dispersed ZrO_2 species (although not necessarily well-integrated to tetrahedral SiO_2 network) at any content studied.

2.4. FTIR Spectroscopy

Peak at around 1060 cm^{-1} corresponded to Si-O-Si asymmetric stretching vibration meanwhile band at ~806 originated by symmetric stretching of aforementioned bonds [15], Figure 1.

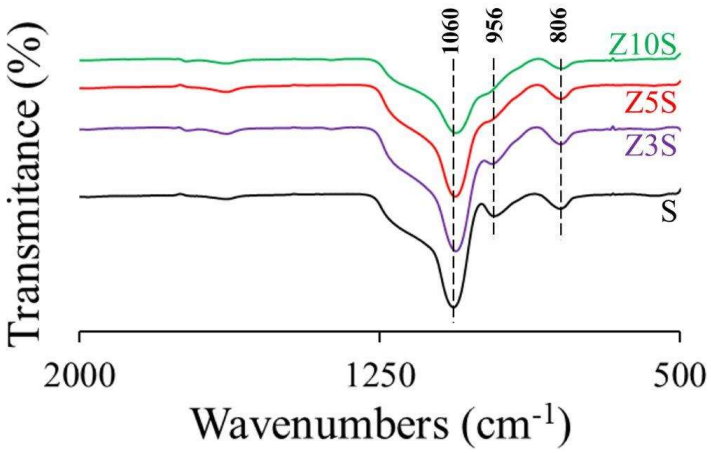

Figure 1. FTIR spectra of pristine SBA-15 and various Zr-modified materials at several nominal contents.

Meanwhile, non-bridged Si-OH stretching vibration [15] was observed at 956 cm^{-1} in pristine SBA-15 (S). This signal could present blue-shifts depending on interaction of those silanols to dopants [6, 16]. Even more, Dong et al. [15] reported disappearance of that signal after Zr deposition, being that attributed to Si-OH and Zr-OH groups association pointing out to Si-O-Zr linkages formation. In our case, progressive diminution in signal intensity was registered, as function of Zr concentration (Figure 1), However, that did not necessarily imply effective integration of totality of zirconium into the mesoporous silica network. As mentioned, interaction could take place on silica surface. Adjusting pH to less acidic conditions have allowed enhanced degree of heteroatoms (Al and Ti) integration in SBA-15 when those species have been directly added during mesoporous matrix synthesis [17]. However, in Zr-modified materials rather acceptable integration has been registered (Zr/Si=0.1, 13 wt%), even in materials prepared without augmented pH [18], although, again, pH adjustment was reflected in augmented zirconium-silica interaction. In our samples acceptable integration of zirconium into the SBA-15 matrices (although not necessarily in the walls) was also observed (Table 1 and Figure 1), mainly in the case of solids of higher Zr content. However, that behavior is clearly dependent on properties of heteroatoms to be inserted. For instance, in the opposite to that found in this investigation La could not be integrated to mesoporous silica solids at any content [6]. The rationale was that very acidic pH conditions during condensation stage of SBA-

 doi:10.20944/preprints202410.2582.v1

15 synthesis do not favor oxo form of heteroatomic species which remained as cationic ones precluding their proper integration to SBA-walls [18, 19].

2.5. UV-Vis Spectroscopy

As expected, SBA-15 (S) did not absorb in the studied UV region [19], Figure 2. Absorption band at energies beyond that corresponding to electromagnetic radiation related to 220 nm could be due to Ligand-Metal Charge Transfer (LMCT) of tetrahedral oxidic Zr species, meanwhile absorption maximum centered at approximately 272 nm could be provoked by Zr^{4+} in other coordination states. Those facts strongly suggested that the former peak originated in framework zirconia integrated to mesoporous silica tetrahedral network whereas the latter evidenced extra-framework species. Considering that, it seemed that Z10S contained the highest proportion of Zi well-integrated in SBA-15 walls, although important proportion could be also as ZrO_2 segregated domains. The later species that showed strong absorption at 272 nm could be provoked by LMCT O^{2-} to Zr^{4+} in octahedral coordination [19]. All in all, our UV spectra results pointed out to coexistence of framework and extra-framework Zr^{4+} as well.

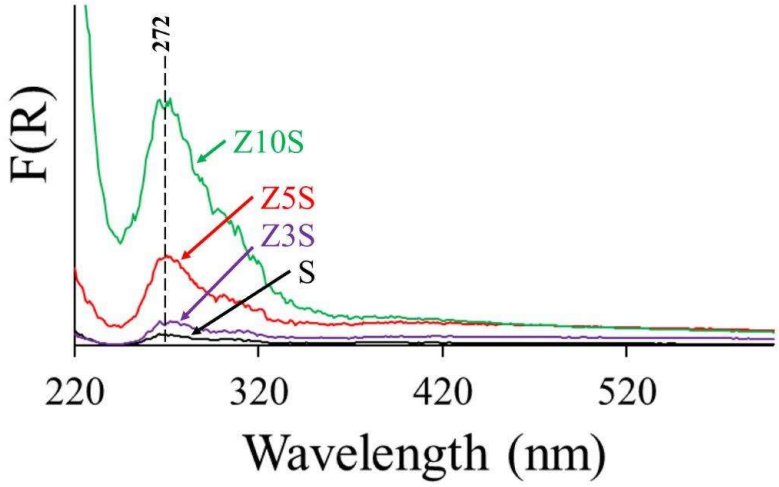

Figure 2. UV-vis spectra of pristine SBA-15 and various Zr-modified materials at several nominal contents.

2.6. HR-TEM

Well-ordered structure with uniform channels along pores axes was clearly observed in pristine SBA-15 solids (Figure 3 (a)), in full agreement with previous reports [20]. As zirconium content in studied formulations progressively increased, amorphous (Figure S2) segregated ZrO_2 domains were evidenced (Figure 3 (b)-(d)), in accordance with that registered by UV spectroscopy (Figure 2).

 doi:10.20944/preprints202410.2582.v1

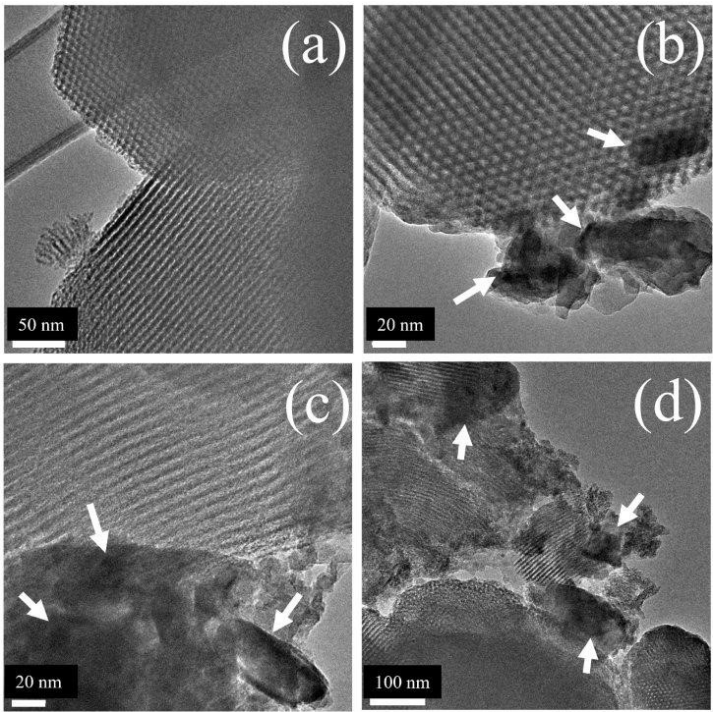

Figure 3. Micrographs of SBA-15-based materials prepared. (a) S; (b) Z3S; (c) Z5S; (d) Z10S. Arrows: ZrO_2 domains.

Note that in all solids SBA-15 mesostructure remained well-ordered, differently to that reported by Colmenares-Zerpa et al. [19] who found that Zr direct addition (Zr/Si=0.1, ~13 wt% Zr, not adjusted pH) resulted in significant SBA-15 structural losses in solids prepared from $ZrO(NO_3)_2 \bullet xH_2O$, suggesting important role of precursor salt used. Supporting that notion mesoporous network ordering was well-kept in the case of solids synthesized from $Zr(SO_4)_2$ (at Zr/Si=0.1) [21]. In our case, extant segregated ZrO_2 domains formation could be favored by distinctive hydrolysis rate of Zr and Si precursors (tetraethyl orthosilicate and $ZrOCl_2 \bullet 8H_2O$, respectively), under synthesis conditions used [6].

2.7. NH_3 Thermodesorption

Weak signal at 120 °C in pristine SBA-15 (S) profile could be related to physisorbed NH_3 and very weak acid sites [4, 6], Figure 4.

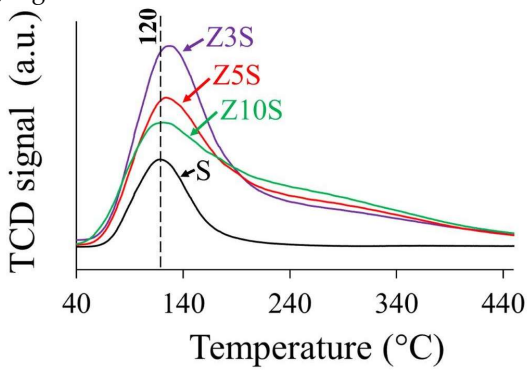

Figure 4. NH_3 TPD profiles of various studied materials at different nominal Zr contents.

Amount and strength of acidic sites significantly enhanced in Zr-modified materials. Acid sites strength was arbitrarily divided according to desorption temperature (T_d), namely weak-medium (80

 doi:10.20944/preprints202410.2582.v1

°C<T_d<250 °C) and strong (250 °C<T_d<380 °C), where most of the sites on Zr-modified solids were not strong (Table 2).

Table 2. Acidic properties (as determined by NH_3 TPD) of various studied formulations.

Sample	Weak-medium	Strong	Total amount (a. u.)·g^{-1}	Total amount (a. u.)·m^{-2}
S	1514830	130032	1644862	2184
Z3S	4494460	1045389	5539849	6121
Z5S	3855059	1760870	5615929	8900
Z10S	4141474	882847	5024321	6585

a.u.: area units, from corresponding TPD profiles integration, Figure 4.

Although the used technique did not allow differentiation between protonic and Lewis sites, Colmenares-Zerpa et al. [19] found, by pyridine FTIR, that approximately 35-40% of Zr-modified solids (Si/Zr=2, 5 and 10, prepared through either direct heteroatom addition during silica synthesis or pH adjusted protocol) total acid sites corresponded to Brønsted ones. Thus, a similar rationale could be applied extrapolating that to our case. As it is known that zirconia possesses just Lewis acidity related to coordinatively unsaturated sites [1], protonic centers creation could be attributed to components interaction through Zr-O-Si linkages. On per mass basis, Z5S had the largest number of total sites, Table 2. Total acidity was not directly related to Zr content in solids as combination of zirconium concentration (Table 1) and dispersion (Figure 3) could strongly influence observed trend. All in all, total acidity of Zr-containing samples was not very different from one to another. The lower population of sites on Z10S could probably be provoked by diminished dispersion as to that of the other solids (Figure 3 (d)). Similar tendency (significantly augmented acidity originated by extant framework and extra-framework ZrO_2 domains) was observed by Chen at al. [4] who studied series of SBA-15 solids modified by direct addition (during mesoporous silica matrix synthesis) of precursors of equimolar MgO-ZrO_2 mixture at high content (10-40 wt%). In surface area basis, the largest basicity was observed, again, for the Z5S formulation. Table 2.

2.8. CO_2 Thermodesorption

SBA-14 (S) just showed a small signal (95 °C) attributed to physisorbed CO_2 species [6, 22]. The surface basic properties of the studied materials were estimated by integrating the area of corresponding TPD profiles, Figure 5. Similarly to that found regarding acidity trends, basicity (number of sites and their strength) was significantly enhanced by Zr addition. However, most of those centers were either weak or of medium strength. The former could be related to bicarbonates formed by CO_2 adsorption on low-strength basic surface hydroxyls [23], meanwhile the latter bidentate carbonates could be formed on Lewis acid-base pairs (Zr-O^{2-}) [23], Scheme S1.

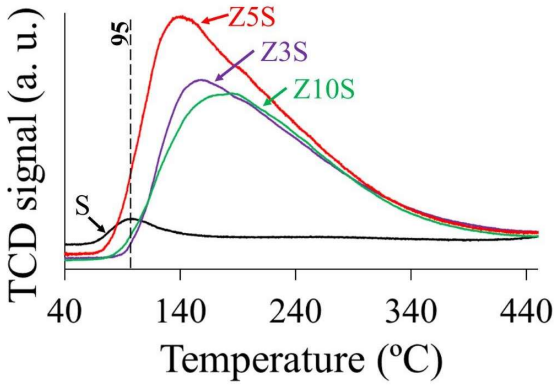

Figure 5. CO_2 TPD profiles of various studied materials at different nominal Zr contents.

 doi:10.20944/preprints202410.2582.v1

Zr addition resulted in basic sites amount increased by almost one order of magnitude being Z5S the sample with the highest sites population, Table 3. In both bases (per mass or per surface area unit) tendencies were similar, where Z5S was the solid of the largest basicity, Table 3. Again, not direct relationship with zirconia content in solids was found.

Table 3. Basic properties (as determined by CO_2 TPD) of various studied formulations.

Sample	Weak-medium	Strong	Total amount (a. u.)·g^{-1}	Total amount (a. u.)·m^{-2}
S	148065	0	148065	197
Z3S	965209	346446	1311655	1449
Z5S	1233922	398474	1632396	2587
Z10S	993136	374776	1367912	1793

a.u.: area units, from corresponding TPD profiles integration, Figure 5.

2.9. Acidic/Basic Properties

Amount (and strength) of SBA-15 surface acid and basic sites were significantly enhanced by extant Zr (Figures 4 and 5, respectively), as observed in Figure 6 where mesoporous silica was used as reference. Also, both protonic (related to Zr-O-Si bonds, framework sites) and Lewis (CUS, extra-framework zirconia) could be present on binary formulations.

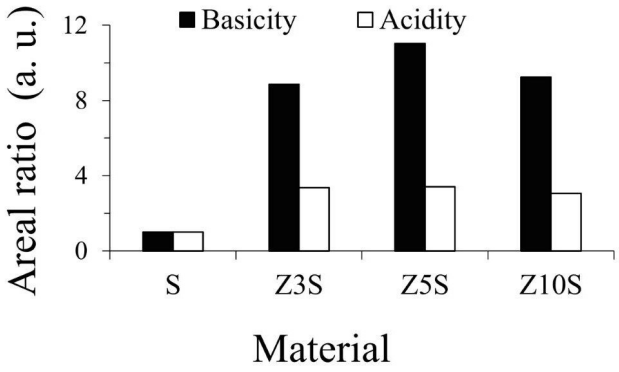

Figure 6. Relative ratio of total acid and basic sites (as determined from NH_3 and CO_2 TPD profiles, respectively) of various studied materials at different nominal Zr contents. SBA-15, (S) as reference.

The effect of zirconium doping was especially notable regarding medium-weak basic sites, Figures 5 and 6. It seemed that the proportion of basic sites were lower than acidic ones, Figure 7.

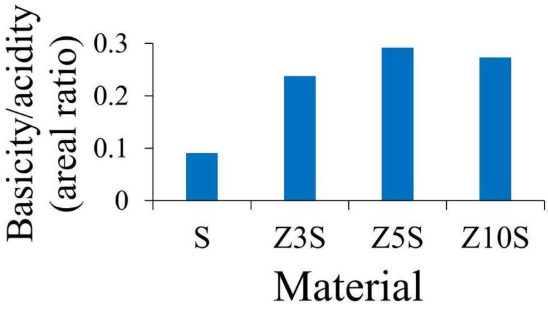

Figure 7. Total basic to acid sites (as determined from CO_2 and NH_3 TPD profiles, respectively) ratio of various studied materials at different nominal Zr contents.

 doi:10.20944/preprints202410.2582.v1

However, it is worth nothing that the last comparison was carried out in area units from TCD signals integration. Thus, that was affected by distinctive thermal conductivity of NH_3 and CO_2 (~2.6x10^{-3} and ~16.1 x10^{-3}, both in W m^{-1} K^{-1}, respectively). In any case, the existence of acid-basic pairs on Zr-modified SBA-15 was proven. Note that the synthesis method followed to prepare binary materials was quite simple and just included a single modifier (section 3.1). However, by utilizing pH-adjusted preparation technique, proportion of framework Zr (inserted in SBA-15 mesoporous network) could be increased [18-19], that being reflected in augmented protonic acidity (originated by higher proportion of Zr-O-Si bonds). Thus, the possibility of finely tuning corresponding amphoteric properties could be feasible. Santacesaria et al. have reported [24] on the relevance of acid-basic pair on Y decationized zeolite applied in ethyl alcohol dehydration where proposed reaction mechanism required of vicinal acid-basic sites. Although the former were able to catalyze dehydration, reaction rate was increased by one order of magnitude by simultaneous presence of the latter ones. It was assumed that carbocation formation (on acid centers) was corresponding limiting step

Also, it was hypothesized that basic centers were required to stabilize carbocation through precursor [24], Scheme S2. Also, amphoteric solids (containing Lewis acid-base pairs) have been recently applied as catalysts to produce biodiesel through fatty acid methyl esters (FAME) [27, 28], where Jatropha curcas biodiesel yield was 100%. These results underline the relevance of those solids in the ongoing energy transition.

In our case, strong acidity was absent on Zr- containing solids. Avoidance of those centers could be very relevant as their existence has been linked to disintegration [27] and coking reactions [28].

Last but not least, corresponding catalytic tests of our Z-modified SBA-15 solids in reactions that demand amphoteric properties are ongoing and will be reported in due course.

3. Experimental

3.1. Materials Synthesis

Zr-Modified SBA-15

To prepare SBA-15 (S) method utilized in [9] was used. Reactants and corresponding amounts of them were as previously detailed [10]. Zr-modified materials (at 3, 5 and 10 wt%, ZxS, x; Zr nominal content) were prepared by directly adding pertinent amounts of $ZrOCl_2 \bullet 8H_2O$, similarly to that carried out in [6], regarding La-containing precursor.

3.2. Materials Characterization

Texture (surface area, pore size distribution (PSD) and pore volume) and structural order of various solids were studied by N_2 physisorption and X-ray diffraction, respectively. Corresponding details could be found elsewhere [6]. Fourier transform infrared (FTIR) spectra of prepared materials were obtained by using Perkin Elmer Frontier equipment. UV-vis DRS spectra of several studied samples were acquired through Shimadzu UV-2600 equipment in the 200-600 nm wavelength range. Surface acidity and basicity of various materials were determined by temperature-programmed desorption (TPD) of NH_3 and CO_2, as described in [6] Compositional analyses were carried out by EDS (Energy-Dispersive X-ray Spectroscopy) apparatus attached to scanning electron microscopy (SEM), JEOL JSM-6010LA (JEOL, Tokyo, Japan) operating at 20 kV accelerating voltage, The materials were characterized by high-resolution transmission electron microscopy (HR-TEM) in Titan 80-300 microscope with a Schottky-type field emission gun operating at 300 kV. The point resolution and the information limit were better than 0.085 nm. HR-TEM digital images were obtained through CCD camera. Prior to analysis powdered materials were ultrasonically dispersed (ethanol).

4. Conclusions

Simple Zr (nominal 3, 5 and 10 wt%, as $ZrOCl_2 \bullet 8H_2O$) direct addition (n Ph ADJUSTEMENT= during SBA-15 synthesis resulted in binary materials of significantly enhanced amphoteric properties

(as determined by NH_3 and CO_2 TPD titrating acid and basic sites, respective-y).), especially in the case of solid modified by nominal 5 wt% Zr content (actual 3.26 wt%, by EDS). Zirconium was integrated in BOTH framework (as found by FTIR and UV-vis spectroscopies) and extra-framework sites (UV-vis and HRTEM) of mesostructured silica network. Total Zr incorporated to mesoporous silica augmented with nominal content in binary formulations, although it was not necessarily integrated in SBA-15 walls forming Zr-O-Si linkages. Single ZrO_2 domains (framework and extra-framework) provided suitable amphoteric properties due to augmented number and strength of both acid and basic sites, that effect being more notable in solid containing nominal 5 wt% Zr). The obtained binary oxides present great potential to be applied in reactions requiring vicinal non-strong acid-basic pairs (alcohols dehydration, for instance).

References

1. Eom, H.-J.; Kim, M.-S.; Lee, D.-W.; Hong, Y.K.; Jeon, G.; Lee, K.Y. Zirconia catalysts (ZrO_2 and Na-ZrO_2) for the conversion of phenethyl phenyl ether (PPE) in supercritical water. *Appl. Catal. A-Gen* **2015**, 493, 149-157. DOI: 10.1016/j.apcata.2014.12.052.
2. Zeidan, R.K.; Davis. M. E. The effect of acid-base pairing on catalysis: An efficient acid-base functionalized catalyst for aldol condensation. *J. Catal*. **2007**, 247, 2, 379-382. DOI: 10.1016/j.jcat.2007.02.005.
3. Shi, L. Y.; Wang, Y. M.; Ji, A.; Gao, L.; Wang, Y. *In situ* direct bifunctionalization of mesoporous silica SBA-15. *J. Mater. Chem*. **2005**, 15, 1392-1396. DOI: 10.1039/B418014N.
4. Chen, Y.; Han, J.; Zhan, H. Structure and acid-base properties of surface-modified mesoporous silica. *Appl. Surf. Sci.* **2007**, 253, 9400-9406. DOI: 10.1016/j.apsusc.2007.05.083.
5. Derawi, D.; Razak, N.A.A.; Saadon, N.S.; Bar, N.A.; Taufiq-Yap, Y.H. Conversion of palm fatty acid distillate to bio-jet fuel-range hydrocarbons over bimetallic NiCo/SBA-15-NH_2 catalyst. *Fuel* **2025**, 380, 133192. DOI: 10.1016/j.fuel.2024.133192.
6. Morales-Hernández, G; Escobar, J.; Pacheco-Sosa, J. G.; Guzmán-Cruz, M.A.; Torres-Torres, J.G.; del Ángel Vicente, P.; Barrera, M.C.; Santolalla-Vargas, C.E.; Pérez-Vidal, H. La-modified SBA-15 prepared by direct synthesis: importance of determining actual composition. *Catalysts* **2024**, 14(7), 436. DOI: 10.3390/catal14070436.
7. Escobar, J.; Colín-Luna, J.A.; Barrera, M.C. Thioresistant PdPt/Al/SBA-15 for naphthalene hydrogenation. *Ind. Eng. Chem. Res*. **2024**, 63(3), 1248-1260. DOI: 10.1021/acs.iecr.3c02359.
8. Rigney, M.P.; Funkenbush, E.F.; Carr, P.W.Physical and chemical characterization of microporous zirconia. *J. Chrom*. **1990**, 499, 291-304. DOI: 10.1016/S0021-9673(00)96980-2.
9. Flodström, K.; Alfredsson, V. Influence of the block length of triblock copolymers on the formation of mesoporous silica. *Microporous Mesoporous Mater*. **2003**, 59, 167-176. DOI: 10.1016/S1387-1811(03)00308-1.
10. Morales Hernández, G.; Pacheco Sosa, J. G.; Escobar Aguilar, J.; Torres Torres, J.G.; Pérez Vidal, H.; Lunagómez Rocha, M.A.; De la Cruz Romero, D.; del Ángel Vicente, P. Improving platinum dispersion on SBA-15 by titania addition. *Rev. Mex. Ing. Quim.* **2020**, 19(2), 997-1010. DOI: 10.24275/rmiq/Mat821.
11. Kobayashi, T.; Sasaki, T.; Takagi, I.; Moriyama, H. J. Solubility of Zirconium (IV) Hydrous Oxides. *Nucl. Sci. Technol*. **2007**, 44(1), 90-94. DOI: 10.1080/18811248.2007.9711260.
12. Leofanti, S.G.; Padovan, M.; Tozzola, G.; Venturelli, B. Surface area and pore texture of catalysts. *Catal. Today* **1998**, 41, 207-210. DOI: 10.1016/S0920-5861(98)00050-9.
13. Palcheva, R.; Kaluža, L.; Dimitrov, L.; Tyuliev, G.; Avdeev, G.; Jirátová, K.; Spojakina, A. NiMo catalysts supported on the Nb modified mesoporous SBA-15 and HMS: effect of thioglycolic acid addition on HDS. *Appl. Catal. A-Gen* **2016**, 520, 24-34. DOI: 10.1016/j.apcata.2016.04.008.
14. Chevalier, J.; Gremillard, L. The Tetragonal-Monoclinic Transformation in Zirconia:
[1] Lessons Learned and Future Trends. *J. Am. Ceram. Soc*. **2009**, 92, 9, 1901-1920. DOI: 0.1111/j.1551-2916.2009.03278.x.
15. Chang, B.; Fu, J.; Tian,Y.; Dong, X. Mesoporous solid acid catalysts of sulfated zirconia/SBA-15 derived from a vapor-induced hydrolysis route. *Appl. Catal. A-Gen* **2012**, DOI: 10.1016/j.apcata.2012.06.031.
16. Giraldo, L.; Bastidas-Barranco, M.; Moreno-Piraján, J.C. Vapour Phase Hydrogenation of Phenol over Rhodium on SBA-15 and SBA-16. *Molecules* **2014**, 19, 20594-20612. DOI: 10.3390/molecules191220594.
17. Wu, S.; Han, Y.; Zou, Y.C.; Song, J.W.; Zhao, L.; Di, Y.; Liu, S.Z.; Xiao, F.S. Synthesis of Heteroatom Substituted SBA-15 by the "pH-Adjusting" Method. *Chem. Mater.* **2004**, 16, 486-492. DOI: 10.1021/cm0343857.
18. Colmenares-Zerpa, J.; Chimentão, R.J.; Gispert-Guirado, F.; Peixoto, A.F.; Llorca, J. Preparation of SBA-15 and Zr-SBA-15 materials by direct-synthesis and pH-adjustment methods. *Mater. Lett*. **2021**, 301, 130326. DOI: 10.1016/j.matlet.2021.130326.
19. Colmenares-Zerpa, J.; Gajardo, J.; Peixoto, A.F.; Silva, D.S.A.; Silva, J.A.; Gispert-Guirado, F.; Llorca, J.; Urquieta-Gonzalez, E.A.; Santos, J.B.O.; Chimentão, R.J.; High zirconium loads in Zr-SBA-15 mesoporous

materials prepared by direct-synthesis and pH-adjusting approaches. *J. Solid State Chem*. **2022**, 312, 123296. DOI: [10.1016/j.jssc.2022.123296.

20. Guo, X.; Feng, Y.; Ma, L.; Gao, D.; Jing, J.; Yu, J.; Sun, H.; Gong, H.; Zhang, Y. Phosphoryl functionalized mesoporous silica for uranium adsorption. *Appl. Surf. Sci*. **2017**, 402, 53-60. DOI: 10.1016/j.apsusc.2017.01.050.
21. Qiang, T.; Zhao, J.; Li, J. Direct synthesis of homogeneous Zr-doped SBA-15 mesoporous silica via masking zirconium sulfate. *Microporous Mesoporous Mater*. **2018**, 257, 162-174. DOI: 10.1016/j.micromeso.2017.08.041.
22. Terrab, I.; Ouargli, R.; Boukoussa, B.; Ghomari, K., Hamacha, R.: Roy, R.; Azzouz, A.; Bengueddach, A. *Res Chem. Intermed*. **2017**, 43, 3775-3786. DOI: 10.1007/s11164-016-2846-7.
23. Di Cosimo, J.I.; Diez, V.K.; Xu, M.; Iglesia, E.; Apesteguia, C.R. Structure and Surface and Catalytic Properties of Mg-Al Basic Oxides. **J. Catal**. **1998**, 178 (2), 499-510. DOI: 0.1016/j.jssc.2022.123296.
24. Santacesaria, E.; Gelosa, D.; Giorgi, E.; Carrà S. Role of basic and acid sites in the bimolecular dehydration of alcohols catalyzed by HY zeolite. *J. Catal*. **1984**, 90, 1, 1-9. DOI: 10.1016/0021-9517(84)90077-0.
25. Zhang, Z.; Meng, P.; Luo, H.; Pei, Z.; Lu, X. Lewis Acid-Base Site-Assisted In Situ Transesterification Catalysis to Produce Biodiesel. *Catalysts* **2024**, 14(10), 731. DOI: 10.3390/catal14100731.
26. Wang, Y.-T.; Fang, Z.; Yang, X.-X.; Yang, Y.-T.; Luo, J.; Xu, K.; Bao, G.-R. One-step production of biodiesel from Jatropha oils with high acid value at low temperature by magnetic acid-base amphoteric nanoparticles. ***Chem. Eng. J***. **2018**, 348, 929-939. DOI:10.1016/j.cej.2018.05.039.
27. Dai, W.; Zhang, L.; Liu, R.; Wu, G.; Guan, N.; Li, L. Plate-Like ZSM-5 Zeolites as Robust Catalysts for the Cracking of Hydrocarbons. *ACS Appl. Mater. Interfaces* **2022**, 14, 9, 11415-11424. DOI: 10.1021/acsami.1c23614.
28. Venezia, A. M.; Murania, R.; La Parola, V.; Pawelec, B.; Fierro,J. L. G. Post-synthesis alumination of MCM-41: Effect of the acidity on the HDS activity of supported Pd Catalysts. *Appl. Catal. A-Gen* **2010**, 383 (1-2), 211-216. DOI: 10.1016/j.apcata.2010.06.001.